SUPPORTING INFORMATION

Automated and Material-Sparing Workflow for the Measurement of Crystal Nucleation and Growth Kinetics

Ryan J. Arruda,[†] Paul A.J. Cally,[†] Anthony Wylie,[†] Nisha Shah,[†] Ibrahim Joel,[†] Zachary A. Leff,[†] Alexander Clark,[†] Griffin Fountain,[†] Layane Neves,[†] Joseph Kratz,[†] Alpana A. Thorat,[‡] Ivan Marziano,[§] Peter R. Rose,[‡] Kevin P. Girard,[‡] Gerard Capellades[†,]*

[†] *Department of Chemical Engineering, Rowan University, Glassboro, New Jersey 08028, United States*

[‡] *Pfizer Worldwide Research and Development, Groton, Connecticut 06340, United States*

[§] *Pfizer Worldwide Research and Development, Sandwich, Kent CT13 9NJ, United Kingdom*

***Corresponding author e-mail:** capellades@rowan.edu

Mathematical Models for Parameter Estimation

This section includes a complete description of the models utilized to estimate the kinetic parameters for nucleation and crystal growth from imaging trends in the Technobis Crystalline. While the system operates as a batch cooling crystallizer and thus follows well-established population balances for relating kinetics to particle size and yield, there was a need to adapt those models to fit with a projected sub-sample of the crystallizing suspension as captured on camera.

The description is hereby divided in two steps: description of the general crystallization models for batch crystallization, and adaptations made to those models to enable parameter estimation from the Crystalline imaging data.

Batch Crystallization Model

Population Balance (Moments). As discussed in the manuscript, a batch crystallizer with negligible agglomeration or breakage presents moment equations with the form:[1]

$$\frac{d\mu_j}{dt} = 0^j B + jG\mu_{j-1} \tag{S1}$$

Where μ_j $(\mu m^j/g)$ *represents the j'th moment,* B $(g^{-1}s^{-1})$ *is the rate of crystal nucleation, and* G $(\mu m/s)$ *is the unidimensional crystal growth rate, projected as the change in the observed dimension* L_{cryst} (μm) *over time.*

Phase Balance. The modeled system is a closed batch crystallizer with a constant composition. The total concentrations of individual components in the crystallizer (e.g. solute, solvent, antisolvent, impurities) can be expressed as mass fractions ($w_{o,i}, g/g\ suspension$) for each component i. Their concentrations in the solid phase are described by their suspension densities ($M_{T,i}, g/g\ suspension$). The concentration of a component i in the mother liquor ($w_{ml,i}, g/g\ solution$) is thus the total concentration of that component in the mixture minus its concentration as a solid, correcting the denominator units by the mass% of the sample that is liquid (1 – total solids concentration). The component phase balance is thus expressed by Equation S2.

$$w_{o,i} = w_{ml,i}\left(1 - \sum M_{T,i}\right) + M_{T,i} \tag{S2}$$

For many systems, the only solids concentration that may have a significant value would be that of the solute ($M_{T,s}$), as impurities tend to incorporate in small levels and solvents may not end up in the crystal lattice. If a system presents hydrates or solvates, the solvent inclusion in the lattice can be quantified with the solvent's solids concentration, and calculated based on the stoichiometry of that incorporation:

$$M_{T,i} = S_i \frac{MW_i}{MW_S} M_{T,s} \tag{S3}$$

Where S_i $(mol\ solvent/mol\ solute)$ *is solvent i's solvation factor for the crystal form, and* MW_i *is the molar mass of the solvent i and the solute s.*

The mass of crystallized solute can be obtained from the third moment of the crystal population, corrected by crystal shape (k_v) and using the crystals' density ($\rho_c, g/\mu m^3$) to convert from volume to mass:[1,2]

$$M_{T,s} = k_v \rho_c \mu_3 \tag{S4}$$

This expression assumes that all crystals have a same crystal habit, and thus they can be characterized from unidimensional populations and using a single crystal shape factor (k_v).

Solubility and Supersaturation. Multiple expressions are used for supersaturation in industrial crystallization, primarily as a function of mother liquor concentration and solubility. Most of them come from approximations of the thermodynamic definition of supersaturation for molecular solutes, and some bring unnecessary assumptions that lead to significant prediction errors. In a prior publication, we discussed those simplifications and numerically demonstrated the consequences of oversimplifying the thermodynamic expression for typical industrial systems.[3] We also provided with a method to estimate thermodynamic supersaturations based on solubility curves and solid-state properties, partially addressing the challenges to led to some of those simplifications in the first place. The model in this work will be based on the thermodynamic expression for supersaturation ($\sigma, dimensionless$), shown in Equation S5, and uses the methods to estimate activity coefficients presented in recent literature.[3,4]

$$\sigma = \ln\left(\frac{\gamma x}{\gamma_{sat} x_{sat}}\right) \tag{S5}$$

Where $x\ (mol/mol\ solution)$ and $x_{sat}\ (mol/mol\ solution)$ are the mole fraction mother liquor concentration and solubility, respectively. γ and γ_{sat} are dimensionless activity coefficients for the supersaturated solution and the equivalent saturated state, respectively.

The solute's mole fraction concentration can be obtained from its mass fraction mother liquor concentration $w_{ml,s}$ using the molar masses of the solute and solution:

$$x = \frac{w_{ml,s}/MW_S}{\sum_{NC} w_{ml,i}/MW_i} \tag{6}$$

The choice of solubility model (x_{sat}) is highly system-dependent and multiple expressions can directly fit in this model, as long as they follow the requirements below:

- The expression takes temperature as one of its inputs and provides solubilities as mole fractions in total solution basis (mol solute / mol solution).
- The expression is accurate within the temperature range between the crystallization temperature and the saturation temperature of the highest investigated concentration.

Empirical models not based on the general solubility equation or Van't Hoff's solubility expression are preferred. This is because the general solubility equation is already used to estimate activity coefficients from the empirical values. The general solubility equation[2] would cancel out in Equation S8, and Van't Hoff is a simplification of the same.

In this work, we have used an empirical model for solubility, following Equation S7.

$$x_{sat} = \alpha \cdot \exp\left(\beta T\right) \tag{S7}$$

Where $\alpha\ (mol/mol)$ and $\beta (K^{-1})$ are constants and $T\ (K)$ is the crystallization temperature. To calculate the activity coefficient in the saturated state, the general solubility equation is used in Equation S8.[2]

$$\gamma_{sat} = \frac{1}{x_{sat}} \exp\left(-\frac{\Delta H_m}{R T_m} ln\left(\frac{T_m}{T}\right)\right) \quad \text{(S8)}$$

Where $\Delta H_m (kJ/mol)$ is the enthalpy of fusion for the crystalline phase, and $T_m (K)$ is its melting point. Those can be obtained from a single Differential Scanning Calorimetry (DSC) experiment on a small powder sample, or from literature if available.

To estimate the activity coefficient at supersaturated conditions, it is necessary to assume that the coefficient presents a low temperature dependence so that it can be read from the equivalent saturated state. This assumption and method were investigated in detail by Valavi, Svärd, and Rasmuson.[4] An effective temperature (T_e, K), being the saturation temperature for the mother liquor concentration, can be calculated from the solubility curve (Equation S9). Then, the general solubility equation is used to approximate the activity coefficient at supersaturated conditions, from the equivalent coefficient that the system would have at saturation (Equation S10).

$$x = \alpha \cdot \exp(\beta T_e) \quad \text{(S9)}$$

$$\gamma = \frac{1}{x} \exp\left(-\frac{\Delta H_m}{R T_m} ln\left(\frac{T_m}{T_e}\right)\right) \quad \text{(S10)}$$

Kinetics. In industrial crystallization, nucleation and unidimensional growth kinetics are typically modeled by the semi-empirical Equations S11 and S12, respectively.

$$B = k_b \sigma^b M_{T,s}^j \quad \text{(S11)}$$

$$G = k_g \sigma^g \quad \text{(S12)}$$

Where k_b $(g^{-1}s^{-1})$ and k_g $(\mu m/s)$ are constants that depend on temperature, solution composition (including solvents and impurities), and mixing conditions. j, b, g are also constants that define the kinetic orders for suspension density and supersaturation. Those may also be solvent dependent.

As discussed in the manuscript, j generally takes values between 2/3 and 2. b is typically found to have values between 2 and 3. Theoretical models for crystal growth place a first or second order supersaturation dependence ($1 \leq g \leq 2$),[2] and this is supported by most parameter estimation studies.

However, it is important to note that, for most size analysis techniques based on laser diffraction, image analysis, or chord length analysis, the measured crystal size and thus the calculated growth rates depend not just on the size of the crystals, but also on how the technique perceives and calculates crystal size. This includes crystal orientation and shape for imaging-based techniques. The provided equations are semi-empirical and the expected parameters are subjected to those biases. In addition, different studies measure supersaturations using very different equations and assumptions. The value of those parameters is also subject to how changes in supersaturation are tracked, which can lead significant differences in the estimated parameter values.

Summary. We have so far described a state-of-the-art batch crystallization model based on tracking distribution moments. A summary of how the model equations for the batch crystallizer are interconnected is provided in Figure S1.

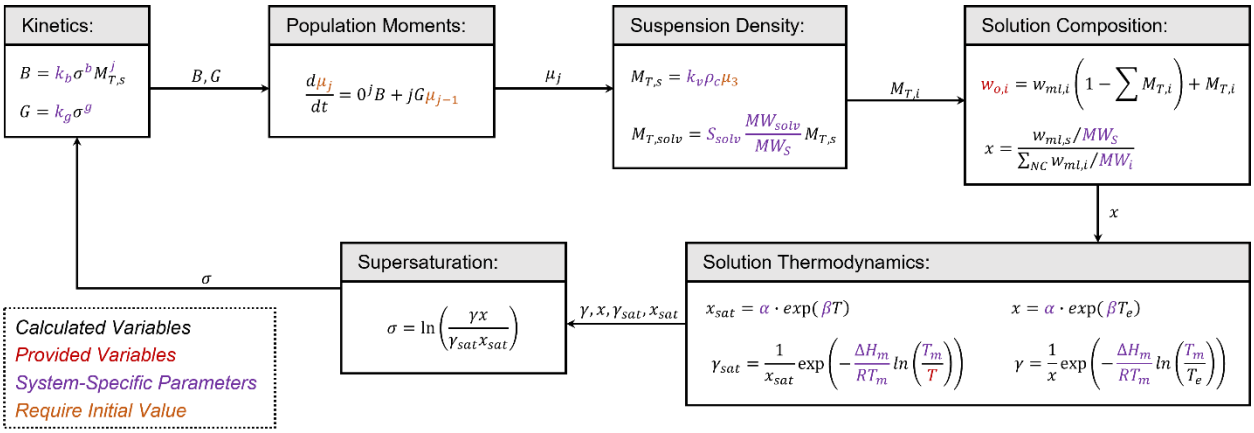

Figure S1. *Summary of the batch crystallization model, before modifications for parameter estimation from Crystalline data. The schematic includes a time-dependent loop that can be solved knowing the initial conditions for the population moments.*

Many of the parameters for the system, like density, molar mass, melting point, or enthalpy of fusion, are known or easily obtained. In addition, solubility parameters can be regressed from experimental solubility data. A typical parameter estimation problem would target to find the missing kinetic parameters for the studied system (k_b, k_g, b, g, j), in this case from Crystalline data. However, none of the calculated variables are obtained as experimental data from the Crystalline. The model thus needs to be adapted to be based on projected crystal moments on camera, instead of total population moments.

Adaptations for Parameter Estimation

Adapting the aforementioned batch crystallization model to be calibrated from Crystalline data requires a new set of assumptions:

1. For dilute systems with negligible crystal overlap on camera, the number of crystals per picture is directly proportional to the total number concentration of crystals in the vial.
2. The system is well-mixed, and the suspension that would be captured in an infinite number of Crystalline pictures would have the same crystal size distribution as the bulk suspension. Note: picture-picture variability is random error that will be seen as noise in the data, but it does not affect the overall trend if the suspension sample is representative (negligible bias error).
3. As it occurs with every other *in situ* technique that tracks projections of crystal size (e.g. FBRM), it is expected that biases in measured particle size translate to all samples, affecting the accuracy of single measurements but not trend-based conclusions (e.g. kinetic comparisons of solutes, solvents, or supersaturations).
4. Crystals have low aspect ratios and can be modeled as cubical. This is a limitation for the method, as crystals with large aspect ratios will present significantly different particle sizes depending on their orientation on camera. Preferred orientations would lead to errors in estimating the second and third moments of the distribution, leading to erroneous kinetics.

Assumptions 1 and 2 require proper mixing in the vial with the absence of classification or floating solute crystals. In addition, they require sufficiently large capture depths so that size classification in the boundary layer near the vial wall does not induce significant errors in the obtained number and size data.

Format of the Raw Data. The Crystalline raw data is in the form of a particle size distribution containing multiple size channels. Once the instrument takes a picture, it measures the area of each crystal, calculates the equivalent circle diameter as the projection of crystal size, and classifies the crystal in a channel based on that diameter. Two independent metrics can be obtained from the distribution of crystals in individual channels: the total crystal number (as the sum of crystals detected in all channels) and the total crystal area (by re-calculating individual crystal areas from the given particle size and summing crystal areas for all channels). Those two metrics are the basis for parameter estimation, as they provide information on nucleation (crystal number) and crystal growth (crystal size). Measurements for crystal size and volume are useful for process understanding, but they are not independent from crystal area and should not be used as independent measurements in parameter estimation.

Projected Moments. As discussed in the manuscript, Crystalline data (number, length, area, volume of crystals in a picture) can be related to the real population moments using the appropriate shape factors as well as a proportionality constant θ $(mg/picture)$ that represents the total mass of suspension captured on camera:

$$N_{tot} = \mu_0 \theta \tag{S13}$$

$$L_{tot} = \mu_1 \theta \tag{S14}$$

$$A_{tot} = k_a \mu_2 \theta \tag{S15}$$

$$V_{tot} = k_v \mu_3 \theta \tag{S16}$$

Where $N_{tot}(crystals/picture)$, $L_{tot}(\mu m/picture)$, $A_{tot}(\mu m^2/picture)$, and $V_{tot}(\mu m^3/picture)$ are the total number, length, area, and volume of the crystals captured on camera, and k_a and k_v are shape factors for area and volume, respectively.

Here, we will make a distinction between the total area of the captured crystals (A_{tot}) and the total crystal area seen by the crystalline (A_{image}), which is a 2D projection of the 3D crystals. Similarly, the Crystalline does not capture crystal volumes directly, but the crystals captured on camera will still have a total volume (V_{tot}). Calculating the total area and volume of the crystals captured on camera requires an additional assumption about the crystal dimension that is hidden in the 2D picture. If the crystals have low aspect ratios, and assuming a random orientation of the crystals in suspension, all dimensions are equally likely to be captured on camera and thus the hidden dimension is similar to those in the 2D projection. For systems with higher aspect ratios, the same crystal can give very different areas depending on how it is oriented, leading to a broader size distribution where not all facets have the same probability to show on camera. The methods hereby presented are valid for cubical or near-cubical crystals only.

Shape Factors for Cubical Crystals. The 2D area of the crystals captured by the Crystalline can be calculated from their provided equivalent circle diameter. For a cubical crystal with a squared 2D projection, it will be assumed that its area projection primarily comes from one of the faces, so that the size of the cube can be approximated from the square root of the projected area (Figure S2). Some error is expected from this assumption, as crystals may be presented with one of the corners facing the camera and project a potentially larger size. However, these differences are expected to be negligible over the course of the experiment, where significant variations in crystal size (often by an order of magnitude) are observed. In addition, orientation-driven errors are not unique of this technique but also found in the estimation of chord length distributions that are currently used in state-of-the-art parameter estimations. As long as these biases are consistent between experiments and the methods are precise, trends can be used in the estimation of kinetic parameters and for comparison between systems.

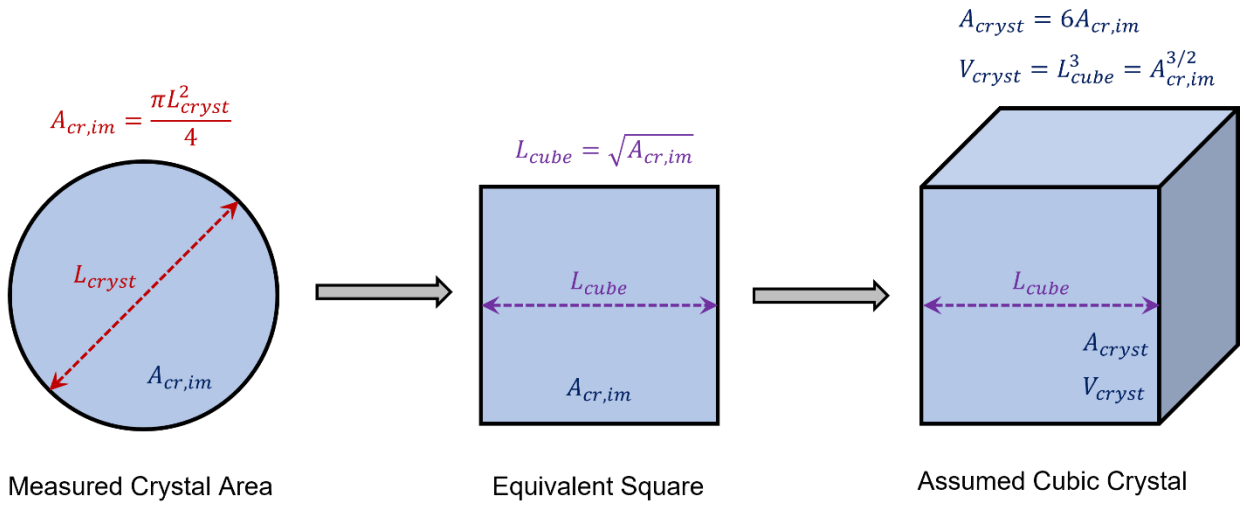

Figure S2. *For a single cubic crystal, size (L_{cryst}) and area ($A_{cr,im}$) captured on the Crystalline, and their relationship with the crystal's total area (A_{cryst}) and volume (V_{cryst}).*

For cubic crystals, the area-based (k_a) and volume-based (k_v) crystal shape factors usually have values of 6 and 1, respectively. However, those are based on the cube size (L_{cube}) as the characteristic dimension.[2] In this work, their values need to be derived accounting for the fact that the characteristic dimension is a circle diameter instead. The actual values can be calculated based on the expected area and volume of a single crystal of size L_{cryst} (Figure S2):

$$A_{cryst} = 6A_{cr,im} = 6\left(\frac{\pi L_{cryst}^2}{4}\right) = k_a L_{cryst}^2 \tag{S17}$$

$$k_a = \frac{3}{2}\pi \tag{S18}$$

$$V_{cryst} = A_{cr,im}^{3/2} = \left(\frac{\pi L_{cryst}^2}{4}\right)^{3/2} = k_v L_{cryst}^3 \tag{S19}$$

$$k_v = \left(\frac{\pi}{4}\right)^{3/2} \tag{S20}$$

By means of the shape factors k_a and k_v, we can now calculate the total area and volume of the crystals captured by the Crystalline, if we know their characteristic size L_{cryst}. For reporting purposes, the instrument does not give the size of every individual crystal. Instead, it classifies each crystal captured on camera into a channel according to its size, ultimately giving a set of counts (N_i) for each size channel (L_i). The total number, length, area, and volume of the crystals in a picture is calculated by equations S21-S24.

$$N_{tot} = \sum_{i\ channels} N_i \tag{S21}$$

$$L_{tot} = \sum_{i\ channels} N_i L_i \tag{S22}$$

$$A_{tot} = \sum_{i\ channels} N_i A_{cryst} = \sum_{i\ channels} N_i \frac{3}{2}\pi L_i^2 \tag{S23}$$

$$V_{tot} = \sum_{i\ channels} N_i V_{cryst} = \sum_{i\ channels} N_i \left(\frac{\pi}{4}\right)^{3/2} L_i^3 \tag{S24}$$

Integration with the Batch Crystallization Model. In order to use Crystalline data for parameter estimation, equation S1 is combined with equations S13-S16 to be expressed as a function of imaging metrics and θ. This results in equations S25-S28.

$$\frac{dN_{tot}}{dt} = B\theta \tag{S25}$$

$$\frac{dL_{tot}}{dt} = GN_{tot} \tag{S26}$$

$$\frac{dA_{tot}}{dt} = 2Gk_a L_{tot} \tag{S27}$$

$$\frac{dV_{tot}}{dt} = 3G\frac{k_v}{k_a} A_{tot} \tag{S28}$$

The solute suspension density can be calculated by substituting equation S16 into equation S4:

$$M_{T,s} = \rho_c \frac{V_{tot}}{\theta} \tag{S29}$$

This model can now be solved as a set of differential equations, adapting the loop from Figure S1 into Figure S3.

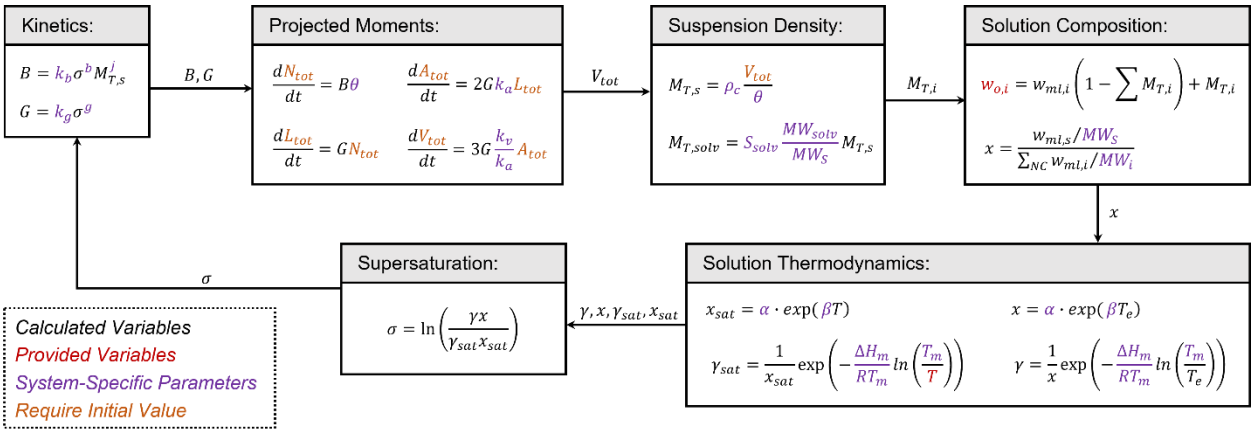

Figure S3. *Summary of the parameter estimation model, adapted to use projected moments from the Crystalline. The schematic includes a time-dependent loop that can be solved knowing the initial conditions for the number, length, area, and volume of crystals on camera.*

For the choice of initial conditions, the simplest choice would be to take the time at which the first crystal was detected as t=0, where the total number, length, area, and volume can be considered negligible. However, this presents two issues:

- The equation for the secondary nucleation rate (Equation S11) requires the solids concentration to be non-zero. Moreover, this is typically based on suspensions with a significant number of crystals, where collisions are frequent. The early stages of the unseeded process, where one or few primary nuclei must build a sufficient suspension density, would have to be simulated by more complex models that are not necessarily representative of the later stages of crystallization.
- Experimental data has a baseline for those variables. Even when no crystals are present, background noise (e.g. from dust particles or dirt in the vial wall) of <10 crystals/picture is often detected by the Crystalline. For the sake of parameter estimation, the initial conditions need to start with those background values. Some error is expected, associated with those measurements potentially misrepresenting the starting conditions for suspension density. It is important to have a clear background to limit this error (e.g. avoiding a dirty vial wall or excessive dust).

In this context, initial conditions for the model are set from a representative time where the total number, length, area, and volume of crystals in a picture are known and non-negligible. Each experiment has a known baseline for the number of crystals per picture (typically around 5) and a maximum value of crystals detected on camera before significant overlap occurs (typically around 250 for the 4 µm/pixel camera). The parameter estimation range is set from these minimum and maximum values, starting when the change is 10% of the total (appr. 25 crystals/picture) and ending when it is 80% (appr. 200 crystals/picture). These values depend on particle size and the background of the sample, so they need to be determined for each experiment. As initial conditions, the moving average for the metrics from appr. 5-10 pictures around t=0 is taken. Systems crystallizing fast (<1 min) may require taking the first data point instead.

gPROMS Nomenclature for the Parameter Estimation Model

Table S1. *Model equations for parameter estimation, including equation size for gPROMS FormulatedProducts.*

Description	Equation form	Size
Component phase balance	$w_{o,i} = w_{ml,i}\left(1 - M_{T,s} - \sum_{NS} M_{T,i}\right) + M_{T,i}$	NC
Solute suspension density	$M_{T,s} = \rho_S \frac{V_{tot}}{\theta} \cdot 10^{-12} mL/\mu m^3$	-
Solvent inclusion in crystals	$M_{T,i} = S_i \frac{MW_i}{MW_S} M_{T,s}$	NS
Solute mol/mol concentration	$x = \frac{w_{ml}}{MW_S \sum_{NC} w_{ml,i}/MW_i}$	-
Solubility in mol/mol	$x_{sat} = \alpha \cdot \exp(\beta T)$	-
Saturation activity	$\gamma_{sat} = \frac{1}{x_{sat}} \exp\left(-\frac{\Delta H_m}{RT_m} ln\left(\frac{T_m}{T}\right)\right)$	-
Effective temperature	$x = \alpha \cdot \exp(\beta T_e)$	-
Solute activity	$\gamma = \frac{1}{x} \exp\left(-\frac{\Delta H_m}{RT_m} ln\left(\frac{T_m}{T_e}\right)\right)$	-
Supersaturation	$\sigma = \ln\left(\frac{\gamma x}{\gamma_{sat} x_{sat}}\right)$	-
Nucleation rate	$B = k_b \cdot \sigma^b \cdot M_{T,s}^j$	-
Growth rate	$G = k_g \cdot \sigma^g$	-
Crystals / picture	$\frac{dN_{tot}}{dt} = B\theta$	-
Crystal length / picture	$\frac{dL_{tot}}{dt} = GN_{tot}$	-
Crystal area / picture	$\frac{dA_{tot}}{dt} = 2Gk_a L_{tot}$	-
Crystal volume / picture	$\frac{dV_{tot}}{dt} = 3G \frac{k_v}{k_a} A_{tot}$	-

Table S2. Model parameters for the equations in Table S1, as they would be implemented to gPROMS FormulatedProducts.

Symbol	Description	Units	gPROMS identifier	Size	Type
NC	System components	-	components	-	ORDERED_SET
NS	Solvents	-	solvents	-	ORDERED_SET
α	Solubility term 1	mol/mol	solubility_1	-	REAL
β	Solubility term 2	K^{-1}	solubility_2	-	REAL
θ	Suspension mass captured on camera	g/picture	theta	-	REAL
b	Nucleation rate order for supersaturation	-	b_order	-	REAL
g	Growth rate order for supersaturation	-	g_order	-	REAL
j	Nucleation rate order for suspension density	-	j_order	-	REAL
k_b	Nucleation rate constant	#/g/s	nuc_constant	-	REAL
k_g	Growth rate constant	µm/s	gr_constant	-	REAL
k_a	Crystal area shape factor	-	A_shape_factor	-	REAL
k_v	Crystal volumetric shape factor	-	V_shape_factor	-	REAL
MW_i	Molar mass of component i	g/mol	molar_mass	NC	REAL
R	Ideal gas constant	kJ/mol/K	R_constant	-	REAL
ρ_i	Density of compound i	g/mL	density	NC	REAL
S_i	Solvation term for solvent i	mol/mol	solvation	NS	REAL
ΔH_m	Enthalpy of fusion for the solute crystals	kJ/mol	enthalpy_fusion	-	REAL
T_m	Melting point for the solute crystals	K	melting_point	-	REAL

Table S3. Model variables for the equations in Table S1, as they would be implemented to gPROMS FormulatedProducts.

Assigned variables Supplied during parameter estimation, with initial conditions

Symbol	Description	Units	gPROMS identifier	Size	Type
B	Solute nucleation rate	$g^{-1}s^{-1}$	rate_nucleation	-	nucleation_rate
G	Linear crystal growth rate	μm/s	rate_growth	-	growth_rate
$M_{T,i}$	Solids concentration of component i	g/g	solids_concentration	NC	solids_concentration
A_{tot}	Area of crystals per picture	μm^2/picture	area_observed	-	crystalarea
L_{tot}	Length of crystals per picture	μm/picture	length_observed	-	crystallength
N_{tot}	Crystals per picture	#/picture	crystals_observed	-	crystalcount
T	Temperature	K	temperature	-	temperature_gFP
T_e	Effective temperature	K	Temperature_eff	-	temperature_gFP
V_{tot}	Volume of crystals per picture	μm^3/picture	volume_observed	-	crystalvolume
$w_{ml,i}$	Mass fraction of compound i in the mother liquor	g/g	ml_conc	NC	mass_fraction_gFP
$w_{o,i}$	Mass fraction of component i in the MSMPR suspension	g/g	mass_fraction_total	NC	mass_fraction_gFP
x	Solute mother liquor concentration in mol/mol	mol/mol	ml_conc_molar	-	mole_fraction_conc
x_{sat}	Solute solubility in mol/mol	mol/mol	solubility_molar	-	mole_fraction_conc
γ	Solute activity coefficient in the supersaturated system	-	activity_coeff	-	activity
γ_{sat}	Solute activity coefficient in the saturated system	-	activity_coeff_sat	-	activity
σ	Solute supersaturation	-	supersaturation	-	supersaturation

Scalability Study

Obtaining scalable kinetics is not the goal of these methods: crystal growth and especially secondary nucleation are sensitive to the inevitable changes in the mixing environment that would occur during scale-up. However, as these methods could become useful in early process development (e.g. screening solvent or temperature effects on kinetics), we want to provide readers with a numerical value to that scalability or the lack thereof. This was investigated using the acetaminophen model system (case study 1 in the manuscript), changing not just crystallizer scale but also configuration, to provide a worst-case scenario. The experimental strategy and models were analogous to those used by Capellades, Wiemeyer, and Myerson in a prior publication.[5]

Two continuous Mixed Suspension Mixed Product Removal (MSMPR) crystallization experiments were conducted in a 120 mL jacketed vessel with overhead stirring. In a typical experiment, a feed containing acetaminophen in 3:1 ethanol:water (by volume) was pumped together with antisolvent (water) at a volumetric ratio of 1:2, reaching a final solvent composition of 25% ethanol and 75% water. The residence time would be set from the individual flow rates, and the system temperature would be maintained at approximately 10 °C by adjusting the temperature of a circulating water bath. This would ensure that the crystallization conditions of temperature and solvent composition matched those used in the experimental screening on the Crystalline.

To mitigate classification during withdrawal, the crystallizer volume was set using a dip pipe and product removal was conducted by means of a programmable peristaltic pump that removes 10% of the crystallizer volume every 10% of a residence time. The MSMPR crystallizer was equipped with a 40 mm overhead propeller operating at 300 rpm. Individual conditions for the two experimental runs are provided in Table S4.

Table S4. Experimental conditions for the MSMPR crystallization experiments.

Condition	Run 1	Run 2
Feed Concentration (mg/g solvent)	285	239
Solute Concentration After Antisolvent Addition (g/L solution)	70.0	60.9
Steady-State Temperature (°C)	12.9	9.8
Residence Time (min)	40	60

Crystallization was monitored using Focused Beam Reflectance Measurements (FBRM S400 Probe, Mettler Toledo) in order to determine steady state. In parallel, mother liquor samples were taken by filtering approximately 4 mL of withdrawn suspension through a 0.45 µm syringe filter. Those samples were analyzed for acetaminophen concentration using High-Performance Liquid Chromatography (HPLC, Fisher Scientific Vanquish™ Core with DAD detector and a 25 cm × 4.6 mm × 5 µm C18 column; acetaminophen absorbance measured at 220 nm). Once the system was at steady-state, small suspension samples were carefully taken from the MSMPR crystallizer using a transfer pipette, and suspended in a saturated solution of acetaminophen in the same solvent system as the crystallizer. This suspension was immediately placed in the Crystalline for particle size analysis. Because the determined growth rates are only a projection of how the analytical equipment sees crystal growth (i.e. equivalent circle diameter for the Crystalline), assessment of size prediction needs to be conducted using the same equipment employed to collect

parameter estimation data. The Crystalline trends were analyzed over time, to ensure that the sample metrics were not time-dependent (this could be indicative of dissolution or growth in the suspension media). In addition, the suspension amount was adjusted so that the number of crystals per picture would not exceed $N_{tot} = 100$ on average. This is to ensure that crystal size measurements are not significantly biased by crystal overlap. Pictures were also inspected to ensure the assumption of a dilute system still holds for the measurements. The Crystalline was programmed to collect appr. 1800 pictures of the equilibrium suspension over a time period of appr. 30 min. The data from those pictures was averaged to compute a volume-based crystal size distribution that would be representative for industrial crystallization. The first two channels (size under 10 µm, or particles around two pixels) were not considered for the analysis as some samples presented a higher background noise. A comparison of the experimental and predicted results for particle size and liquid concentration is provided in Figure S4. Details on the MSMPR model for prediction used can be found in a prior publication.[5]

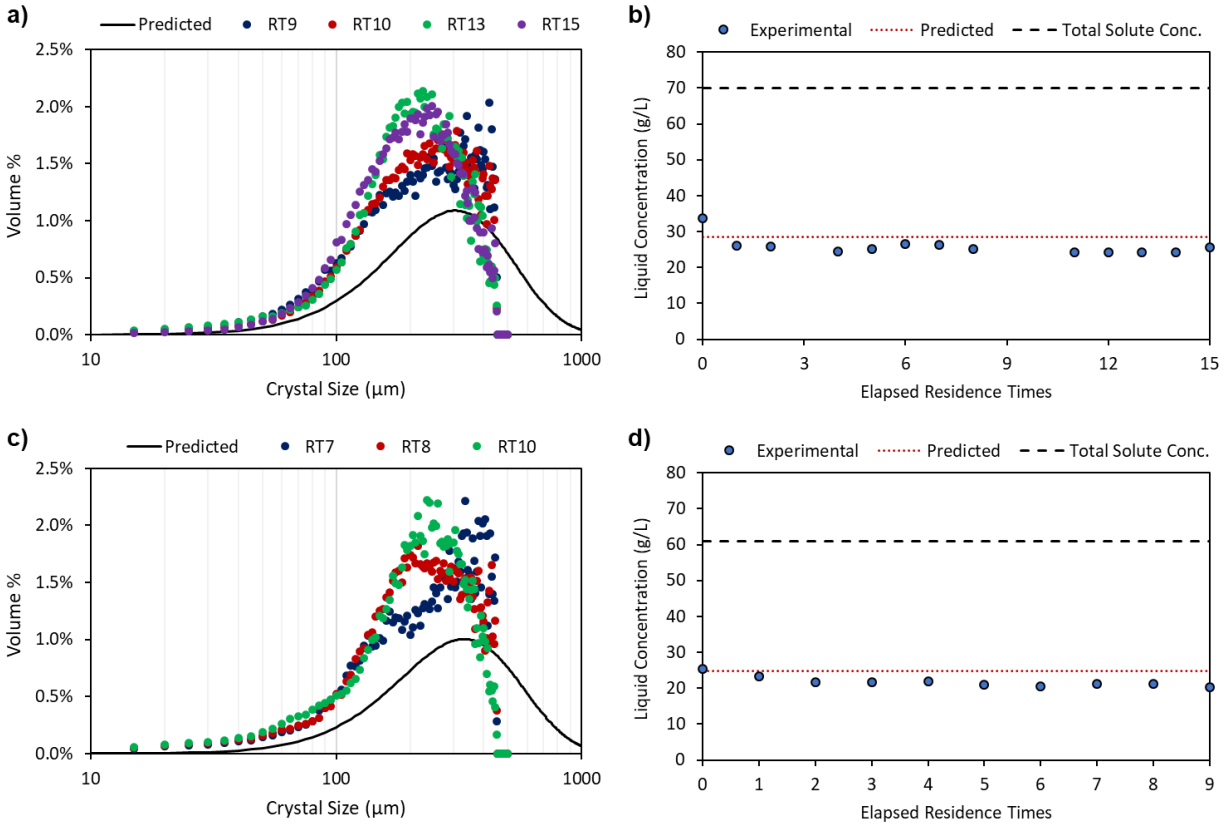

Figure S4. *MSMPR prediction results. a) volume-based crystal size distribution for Run 1. b) steady-state mother liquor concentration for Run 1. c) volume-based crystal size distribution for Run 2. d) steady-state mother liquor concentration for Run 2.*

Crystal size increased from run 1 to run 2, as expected due to the longer residence time and lower supersaturation. A small increase in particle size was predicted by the model, estimating a change in volume-based mean from 412 µm to 446 µm between runs 1 and 2. The predicted yields from the MSMPR model were 59.4% and 59.3% for runs 1 and 2, respectively. While run 2 has a longer residence time and smaller steady-state liquid concentration, it also has a lower feed concentration. The experimental yield values were 64.3% and 65.3% for runs 1 and 2.

Regarding prediction of crystal size, the model overestimates its steady-state value. This could be the result of a change in the crystal nucleation kinetics between the two scales. Note that, because secondary nucleation relies on collisions, different mixing patterns will lead to different rates. Similarly, MSMPR crystallizers operating near-equilibrium will have higher solid concentrations than a batch crystallizer during the first few minutes of crystallization. While the effect of solid concentration is considered during parameter estimation, the data used to train the model is for lower concentrations. Another reason for the difference in values could be the error in measuring large crystal sizes using the Crystalline. The highest size channel offered by the instrument is 500 µm, just over the mean size predicted by the MSMPR model. Larger crystals will not be detected by the instrument, and crystals nearing the upper channels are more likely to fall at the edge of a picture and be removed by the algorithm. The sharp decline in frequency for the experimental results in Figure S4a and Figure S4c indicates that some larger crystals are present but not being measured.

Regarding prediction of mother liquor concentration and yield, the model reasonably predicts that the system will operate near-equilibrium, but this is to be expected for an MSMPR crystallizer with a sufficiently long residence time. Shorter residence times led to fouling, and they were not investigated in more detail. Here, it is also important to note that the MSMPR model converged very close to equilibrium, and that lower concentrations were limited by the estimated solubility value. It is possible that the overprediction is driven by solubility and not kinetics. Especially at these scales, small variations in pump flow rates can lead to changes in solvent composition and slightly change the solubility value. Similarly, the presence of solute in the feed solution already decreases the amount of solvent that is actually pumped in that stream, and the solvent composition will be skewed towards higher antisolvent contents and lower solubilities. Small variations in temperature and solvent composition will change both solubility and kinetics, contributing to a weaker prediction from kinetic values calibrated at fixed conditions.

Overall, these results reinforce the idea that kinetics from these methods should not be used to directly predict the operation of scaled-up systems, especially when particle size prediction is critical. Crystallization kinetics, especially secondary nucleation, change across scales. However, this does not mean that the methods are not valid for process development. A typical approach to the development of industrial crystallizers involves running several experiments at the 100-1000 mL scale, to screen not just for kinetics but also for the effects of temperature, supersaturation, and even solvent on crystallization kinetics. Those dependencies are properties of the solute-solvent system and, as long as liquid composition (e.g. impurity content, or solvent fraction) is kept constant during scale-up, they would be scalable. A system presenting a strong temperature or solvent dependence will present that behavior across scales. It is not necessary to run 10-15 continuous crystallization experiments at the 100 mL scale to obtain values for every crystallization parameter. Instead, one can run a rapid screening to find which temperatures and solvents may work best and define which dependencies will be modeled. Then, 2-3 experiments can be run at the right scale, targeting only the important parameters. Similarly, the use of an automated and standardized approach to measure kinetics has value for laboratories working with multiple compounds. Over time, those laboratories can build internal databases for kinetics in multiple systems, using values that do not depend on the operator or the choice of model. New systems can then be compared to existing systems in the database, to inform the general behavior and select a crystallization strategy for the new compound.

References

(1) Randolph, A. D.; Larson, M. A. *Theory of Particulate Processes - Analysis and Techniques of Continuous Crystallization*; Academic Press, Inc., 1971.

(2) Myerson, A. S.; Edemir, D.; Lee, A. Y. *Handbook of Industrial Crystallization*, Third Edit.; Cambridge University Press, 2019.

(3) Schall, J. M.; Capellades, G.; Myerson, A. S. Methods for Estimating Supersaturation in Antisolvent Crystallization Systems. *CrystEngComm* **2019**, *21*, 5811–5817. https://doi.org/10.1039/c9ce00843h.

(4) Valavi, M.; Svärd, M.; Rasmuson, A. C. Improving Estimates of the Crystallization Driving Force: Investigation into the Dependence on Temperature and Composition of Activity Coefficients in Solution. *Cryst Growth Des* **2016**, *16*, 6951–6960. https://doi.org/10.1021/acs.cgd.6b01137.

(5) Capellades, G.; Wiemeyer, H.; Myerson, A. S. Mixed-Suspension, Mixed-Product Removal Studies of Ciprofloxacin from Pure and Crude Active Pharmaceutical Ingredients: The Role of Impurities on Solubility and Kinetics. *Cryst Growth Des* **2019**, *19* (7), 4008–4018. https://doi.org/10.1021/acs.cgd.9b00400.